

Modelling of Resonant Field Amplification in JET

Yueqiang Liu¹, I.T. Chapman¹, S. Saarelma¹, M.P. Gryaznevich¹, T.C. Hender¹, D.F. Howell¹ and JET-EFDA contributors*

JET-EFDA, Culham Science Centre, Abingdon, OX14 3DB, UK

¹*Euratom/UKAEA Fusion Association, Culham Science Centre, Abingdon, OX14 3DB, UK*

**See the Appendix of F. Romanelli et al., Fusion Energy 2008 (Proc. 22nd Int. Conf. Geneva, 2008) IAEA, (2008)*

1. Introduction. The effects of error fields on the stability and confinement of tokamak plasmas have been known for a long time [1]. Passive or active error field correction, using magnetic coils, has been proved an efficient way to improve the plasma performance in many present tokamaks. It is also foreseen as an important design aspect in ITER. It was, however, only recently realised that the plasma response can play a crucial role in amplifying the external, static magnetic fields, due to the existence of meta-stable, low- n , low frequency MHD modes in the plasma. One example is the resonant field amplification (RFA) caused by the resistive wall mode (RWM), marginally stabilised by the plasma rotation or kinetic effects.

In this work, we model the RFA response by solving the linearly perturbed, single fluid MHD equations as a forcing problem by using the MARS-F code, in which the source term is the coil currents flowing in the error field correction coils (EFCC) in JET. We investigate two types of the plasma response, observed in JET discharges, that occur *before* the plasma pressure reaches the no-wall limit for the ideal kink mode.

2. RFA due to resistive wall modes. For the RFA modelling, we use toroidal equilibria reconstructed from JET pulses. An axi-symmetric, complete, thin shell is used to approximate the conducting wall (vacuum vessel) in JET. The radial and poloidal locations of the EFCC and the sensor coils (close to the wall) are specified according to the experimental geometry. In the JET experiments, the integrated coil signals at a toroidal angle, 90 degrees shifted with respect to the EFCC currents, is used as the RFA response from the plasma. These pick-up signals measure the pure plasma response field (i.e. without the vacuum field produced by the EFCC currents). The same definition of RFA is followed in the MARS-F simulations.

As a motivation, Fig. 1(a) shows the growth rates (solid lines) of the $n = 1$ ideal kink mode, computed for three different JET plasmas. The marginal stability corresponds to the no-wall beta limit, in terms of the normalised beta $\beta_N \equiv \beta(\%)a(m)B_0(T)/I_p(MA)$. Three vertical (dash-dotted) lines indicate the measured $n = 1$ RFA threshold from experiments [2], defined as the β_N value giving the minimum of the curve $|RFA|/\beta_N$ as a function of β_N . We observe a systematic, large downward shift of the RFA-measured thresholds compared to the beta limits according to the ideal MHD theory. This is also confirmed by the MARS-F computations, shown in 1(b). This systematic shift poses difficulties in predicting the beta limit by using the RFA data. A possible remedy is suggested by Fig. 1(c), where we re-define the RFA threshold as β_N value giving the peak value of the logarithmic derivative of the RFA amplitude, as a function of β_N . The new RFA threshold agrees well with the no-wall beta limit.

A more carefully tuned reconstruction procedure does result in a more accurate equilibrium for the JET plasma, which brings reasonable agreements between the experimental data and the modelling results not only for the RFA threshold, but also for the no-wall beta limit. One example is shown in Fig. 2(a), where the equilibrium q profile (the radial location of rational surfaces) is carefully calibrated by matching the measured plasma toroidal rotation frequency

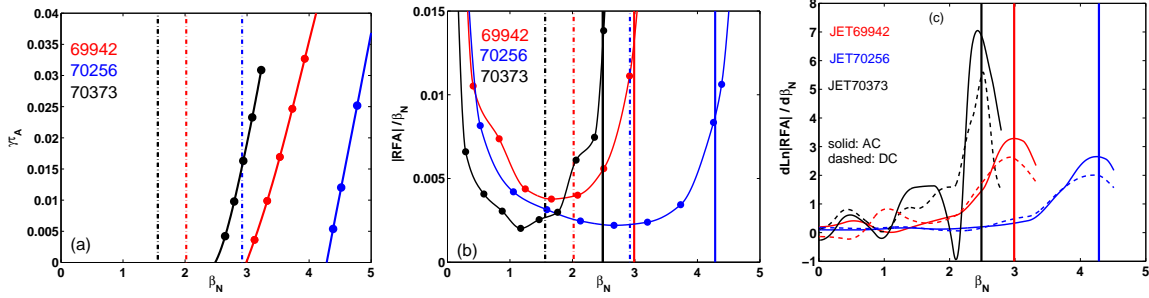


Figure 1: (a) Growth rates (solid) of the $n = 1$ ideal kink mode versus β_N for three JET plasmas. The dash-dotted vertical lines indicate the corresponding $n = 1$ RFA threshold measured in experiments. (b) The MARS-F computed RFA amplitude for these three plasmas. (c) Modelling shows that the logarithmic definition of the RFA thresholds match well the no-wall beta limit.

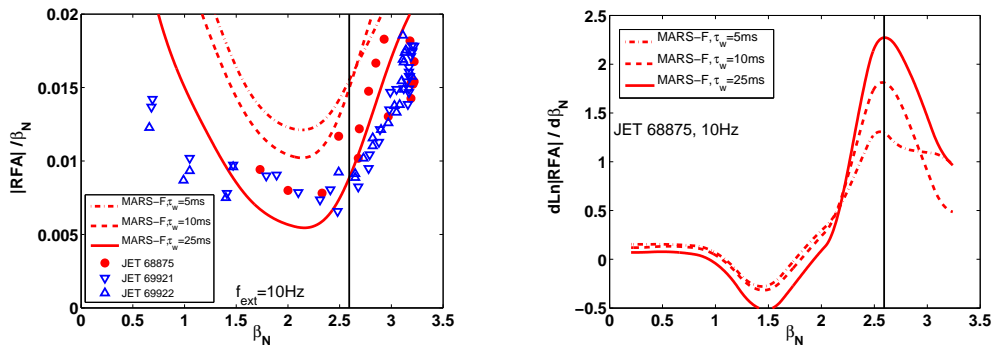


Figure 2: (a) Comparison of the modelled RFA amplitude (curves) with the experimental data (dots) from three similar pulses. Various values of the wall penetration time are assumed in the modelling. The solid vertical line indicates the computed no-wall beta limit. (b) Agreement between the logarithmic RFA threshold and the no-wall limit for the same case.

with the measured MHD (islands) rotation frequency, for JET pulse 68875 [3]. Figure 2(a) compares the computed RFA amplitude (lines), based on a set of equilibria for 68875, with the measured values (dots) from three similar discharges including 68875. In the simulation, we have to vary the wall penetration time τ_w for the 2D thin shell model, in order to approximately take into account the effect of 3D conducting structures located between the plasma surface and the EFCCs. We make this approximation since the MARS-F code can represent only toroidally uniform (i.e. 2D) walls. At a finite EFCC frequency (10Hz in these JET pulses), the induced eddy currents in these 3D conducting structures effectively increase the wall penetration time. We emphasise that a detailed, 3D model of the JET conducting structures may be essential for a quantitative prediction of the RFA amplitude.

Figure 2(a) shows that one can choose an 'equivalent' wall time constant (25ms in this case), for which the simulated RFA amplitude matches well the experimental value. More noticeably, even if we relax the requirement on matching the RFA amplitude (hence the wall time tuning), we still obtain a good agreement between the computed and the measured RFA threshold (about $\beta_N = 2.4$ in this case). According to the stability calculation for the $n = 1$ ideal kink mode, the no-wall beta limit is about 2.6 for the JET plasma 68875. This limit is again well reproduced by the computed RFA response, by evaluating the logarithmic derivative of the RFA amplitude, as shown in Fig. 2(b), which also shows that this definition is not sensitive to the choice of the wall time constant.

Further modelling results also show that the logarithmic definition of the RFA threshold, for

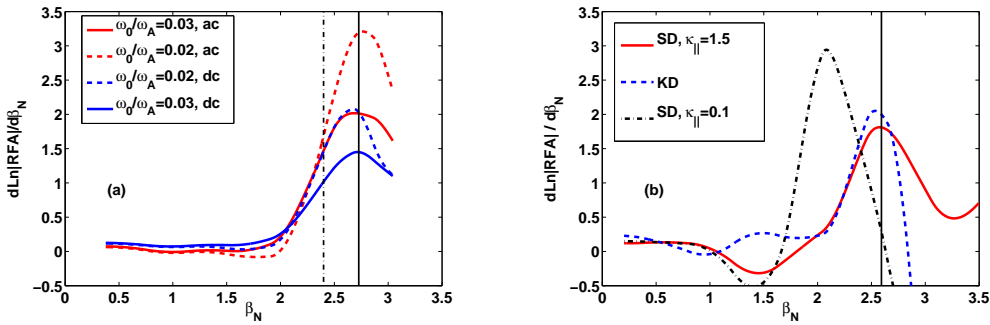


Figure 3: *Robustness of the logarithmic definition of the RFA threshold in predicting the no-wall beta limit. (a) Robustness against variation of the plasma rotation and the external field excitation frequency. (b) Robustness against the RWM damping models with strong damping.*

the purpose of predicting the no-wall beta limit, is robust against the other wall characteristics (e.g. the wall geometry), the plasma rotation speed, the damping models, as well as the plasma equilibrium profiles (e.g. the edge current pedestal). Figure 3(a) shows an example, where the plasma rotation speed is varied. Both dc and ac excitation conditions are considered. The MARS-F computed RFA threshold, according to the new definition, agrees reasonably well with the computed no-wall beta limit in all cases. Fig. 3(b) shows another example, where we compare three cases: a strong parallel sound wave damping (SD, $\kappa_{||} = 1.5$), a weak parallel sound wave damping (SD, $\kappa_{||} = 0.1$), and a drift kinetic damping (KD) model [4]. The sound wave damping model introduces a viscous force to effectively mimic the ion Landau damping of the parallel sound wave [5]. A numerically adjustable coefficient $\kappa_{||}$ is introduced in this model to prescribe the degree of damping. The drift kinetic damping model exploits the mode resonance with the precessional drift of trapped thermal ions and electrons in the full toroidal geometry. The latter model, without any numerical adjustable parameters, provides a strong damping on the resistive wall mode in high beta plasmas. Figure 3(b) shows that, as long as the damping is strong enough, both damping models lead to a good prediction of the no-wall beta limit. On the contrary, a weak damping gives a RFA threshold far below the no-wall limit, and is therefore inadequate for describing the dynamics of the plasma RFA response.

Finally, we point out that it may not be easy to implement the logarithmic technique experimentally in the presence of noise.

3. RFA due to peeling modes. Figure 4(a) shows the plasma RFA response to a standing wave EFCC current at 20Hz in two JET pulses 70199 and 70200. Two peaks occur at β_N values about 2.3 and 2.0 respectively, considerably below the estimated no-wall beta limits (about 2.9 and 2.5 respectively). It is unlikely that these two peaks contain a dominant contribution from the response of the RWM (The RFA response, measured near the no-wall beta limits, is dominantly caused by the stable RWM). Besides, experimental evidence suggests a correlation between these low frequency RFA signals and the ELM (edge localised mode) free period prior to the first ELM [2]. We compute the RFA response of the marginally stable $n = 1$ peeling mode, that offers one possible explanation to the experimental observations. Figure 4(b) shows the typical equilibrium profiles used in the modelling for the ideal peeling mode. Note that a finite current density is artificially maintained and adjusted, in order to obtain unstable/stable peeling modes. Using the profiles shown in Fig. 4(b), we generate a series of equilibria, by varying (slightly) the total plasma current (thus the edge value of the safety factor q , q_a), while keeping the plasma pressure at a low value $\beta_N = 1$, to minimise the response from the RWM. For this series of equilibria, the peeling mode stays stable when the stability parameter

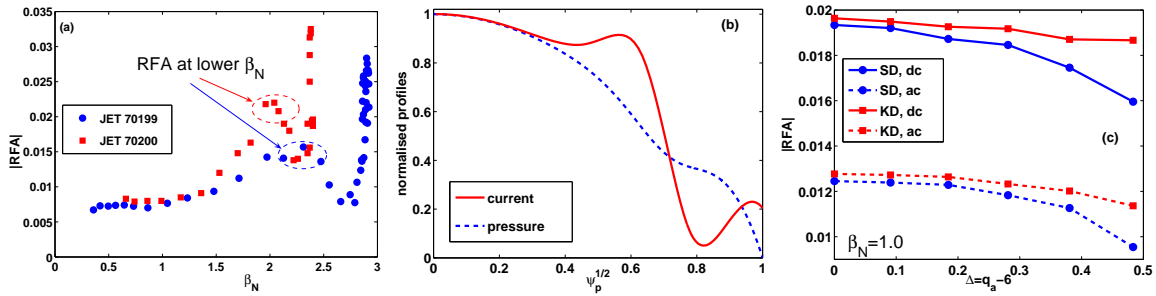


Figure 4: (a) The low-beta RFA response measured in the JET pulses. (b) The plasma equilibrium current and pressure profiles, re-constructed from the pulse 70200 and used in the peeling mode modelling. (c) The RFA response of the stable $n = 1$ peeling mode with sound wave (SD) versus kinetic damping (KD) models, and dc versus ac excitations.

$\Delta \equiv q_a - 6$ exceeds 0. Figure 4(c) shows the computed RFA amplitude versus Δ , with both static and standing wave (with a frequency approximately matching the experimental value) EFCC currents assumed. The computed RFA amplitudes largely agree with the measured RFA peaks shown in Fig. 4(a), with the strongest response occurring at $\Delta = 0$, corresponding to a marginally stable peeling mode. The RFA response of the peeling mode is not sensitive to the damping models, in contrast to the RWM.

We point out that it is difficult to make a direct comparison of the computed RFA with experimental data, due to the fact that, for a given β_N , the value of Δ , which controls the stability of the peeling mode, depends on the precise details of the equilibrium, especially the current profile at the plasma edge. Therefore, the above peeling mode modelling results provide only a *qualitative* explanation of the JET experiments.

4. Conclusion and discussion. The effect of resonant field amplification, due to the response of the low- n MHD modes to the externally applied magnetic fields, is modelled for JET plasmas using the MARS-F code.

For the RWM induced RFA, study is focused on the RFA threshold measured in JET discharges. The simulation results confirm the systematic shift of the RFA onset pressure from the predicted no-wall beta limit by ideal MHD theory. A new technique of using the RFA data to predict the no-wall beta limit is proposed, based on the logarithmic derivative of the RFA amplitude. This technique offers a better way to predict no-wall beta limit. However, it requires accurate low noise RFA measurements from experiments. Some of the RFA peaking, observed in JET discharges during the ELM events at low plasma pressures, is explained by the resonant response of stable $n = 1$ peeling modes, located at the plasma edge.

Acknowledgements. Y.Q. Liu acknowledges many fruitful discussions with Drs. C.G. Gimblett and V.D. Pustovitov during this work. We also thank Drs. H.R. Koslowski and A.W. Morris for valuable suggestions in improving the paper. The JET TF S2 Team is also acknowledged for the experimental data. This work was funded jointly by the United Kingdom Engineering and Physical Sciences Research Council and by the European Communities under the contract of Association between EU-RATOM and UKAEA. The views and opinions expressed herein do not necessarily reflect those of the European Commission.

- [1] Hender T C et al 2007 *Nucl. Fusion* **47** S128; [2] Gryaznevich M P et al 2008 *Plasma Phys. Control. Fusion* **50** 124030; [3] Chapman I T et al 2009 *Plasma Phys. Control. Fusion* **51** 055015; [4] Yueqiang Liu et al 2008 *Phys. Plasmas* **15** 112503; [5] Chu M S et al 1995 *Phys. Plasmas* **2** 2236